Plasma-kinetics perspective on a collisional Ni-like x-ray laser pumped by a single profiled laser pulse

K. A. Janulewicz,* J. Tümmler, G. Priebe, and P. V. Nickles
Max Born Institute, Max-Born-Strasse 2A, D-12489 Berlin, Germany
(Received 22 February 2005; revised manuscript received 27 April 2005; published 27 October 2005)

Some aspects of plasma kinetics in a Ni-like Ag soft x-ray laser have been analyzed, starting from the real shape of the pump laser pulse measured with a third-order correlator. The role for pump energy reduction of a complex pump pulse structure at a low intensity level has been identified, and the modeling results on the gain lifetime correspond well with the length of the output x-ray pulse measured in the experiment.

DOI: 10.1103/PhysRevA.72.043825 PACS number(s): 42.55.Vc, 42.79.Hp, 52.25.Kn, 52.50.Jm

Collisional x-ray lasers, working within the transient inversion scheme and pumped by a combination of two (long/short) separate and well-defined laser pulses, have enabled dramatic reduction in the pump energy, especially for active media including an abundance of Ni-like ions [1,2]. While a reasonable part of this progress can be ascribed to favorable scaling rules for the atomic structure of the Ni-like isoelectronic sequence, the dominant part has been caused by changes in the parameters of the pump process. The low-energy preparatory nanosecond laser pulse ablates a limited amount of the target material, and this facilitates heating by the main (picosecond) laser pulse of reduced energy. Application of longer (a few picoseconds) heating laser pulses improved the efficiency of the collisional absorption process by elongation of the interaction process [3–5]. The balance between the energies included in both parts of the pumping process became of paramount importance for the efficacy of the scheme, as the volume of the ablated material should match the heating capabilities of the main part of the pump pulse.

This traditional variant of the double-pulse pump system has been continuously developed, and the recent qualitative progress was achieved by the demonstration of a Ni-like Ag soft x-ray laser pumped by a single profiled picosecond laser pulse [3]. This scheme offered the lowest pump energy for the laterally irradiated slab targets. The estimated ratio of the gain-length product to the pump energy was 5 J^{-1}, and saturation with the pump energy less than 3 J has been reported [6,7]. It was assumed that such a pump process was possible owing to a low-level background preceeding the main heating pulse, as no separate prepulses were observed in the experiment. The numerical analysis presented in Ref. [4] confirmed the feasibility of such a variant of the transient inversion scheme, and also revealed some physical aspects not observed in the traditional double-pulse pumping scheme. It was found that a low-level component of the pump laser pulse with an energy of $\sim$20 mJ [full width at half maximum (FWHM) 2 ns] is able to ablate a very small amount of the target material, which is subsequently heated by an extended picosecond pulse (FWHM 4–12 ps) to the temperature of 200–300 eV. This temperature is sufficient to excite efficiently by electron impact the lasing levels of a lasant. The experiment and theory showed that an increase in the ablated mass of material was not beneficial for lasing, presumably due to insufficient energy for heating. Low preforming energy moved the lasing area towards a high density plasma. This area converted very quickly to a strongly absorbing region due to cooling by thermal conduction to the massive target. However, the proposed simple shape of the pump laser pulse with a two-step structure (low-level nanosecond background and a picosecond heating pulse) was not able to explain a major contradiction observed in the experiment. The experimental results presented in Ref. [6] showed the width (FWHM) of the output pulse of a silver XRL ($\lambda = 13.9$ nm), recorded with a Kentech x-ray streak camera, in the range of 32±3 ps while typical values in the traditional transient scheme at a comparable pump energy are about 10 ps. Very limited increase in the gain when the traveling wave pump arrangement was used in the experiment supported the assumption of the long-lived gain. Quantitatively, the output x-ray laser (XRL) pulse of the measured length requires even longer gain lifetime. In both the experiment [8] and modeling [4,8], the gain lifetime increased only very weakly with the length of the pump laser pulse. The changes in the background length and its intensity also did not affect the gain lifetime in a notable way. Thus, it was clear that the tradi-

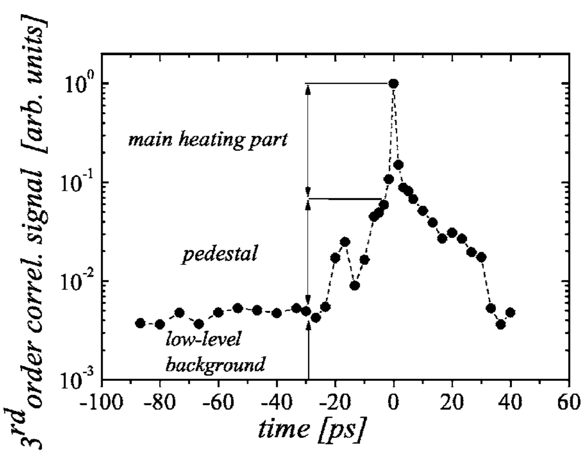

FIG. 1. The correlation trace of the amplified pump laser pulse measured with the OPA (third-order) correlator [9]. Time counting is related to the peak of the heating pulse.

*Electronic address kaj@mbi-berlin.de

 ©2005 The American Physical Society

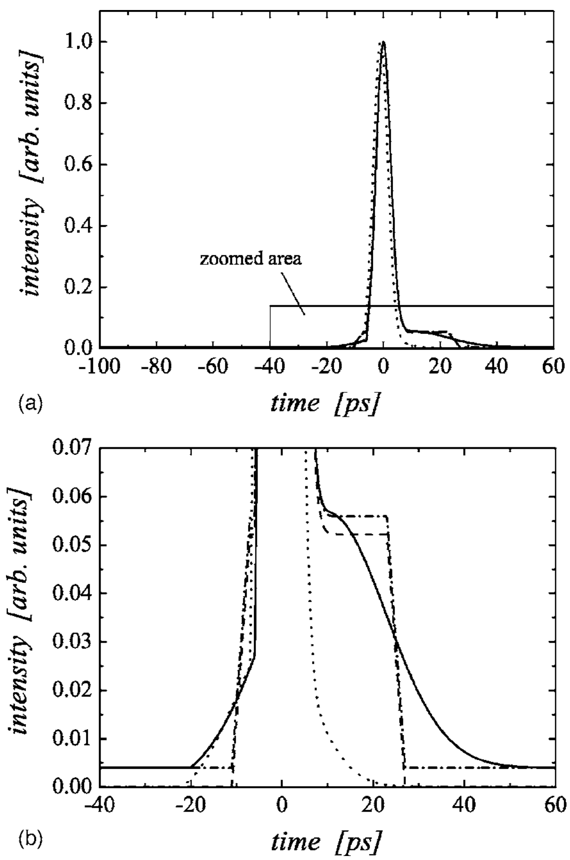

FIG. 2. (a) Modeled shapes of the profiled pump pulse and (b) zoomed pulse structures at the low-energy level. The shape of the pump pulse with an energy of 2.6 J corresponding well to the shape obtained from the third-order correlator measurement is traced with the solid line. Doted line sketches the pump pulse with "steep edges," i.e., without any pedestal on the falling edge. The dashed line shows a pulse with a trapezoidal pedestal and a background level of $10^{-4}I_{\max}$. The dash-dotted line show nearly identic pulse but with the background at a level of one order of magnitude higher. The effect of the dashed and dotted pulse shapes is compared in the simulations.

tional two-step structure of the profiled pump laser pulse is not able to explain the mentioned contradiction, and does not describe correctly the behavior of the XRL output if pumped by a single pulse from our laser driver.

Determining an exact profile of the pump laser pulse became essential for understanding the active medium kinetics. Earlier measurements with an optical streak camera indicated existence of the low-level intensity ramp with the length of at least 500 ps. This was not a reliable value as streak cameras have a low dynamic range ($\sim$30), and they are usually not able to reveal the pulse structure at a level below 1% of the peak intensity [9].

In the present paper we describe the results of numerical simulations on plasma kinetics of a Ni-like Ag x-ray laser pumped by a single, profiled pulse. Modeling was supported by the measurement results on the pump pulse shape performed with an OPA third-order correlator. Comparison between both helped to explain the apparent contradiction between the high value of gain suggesting its transient

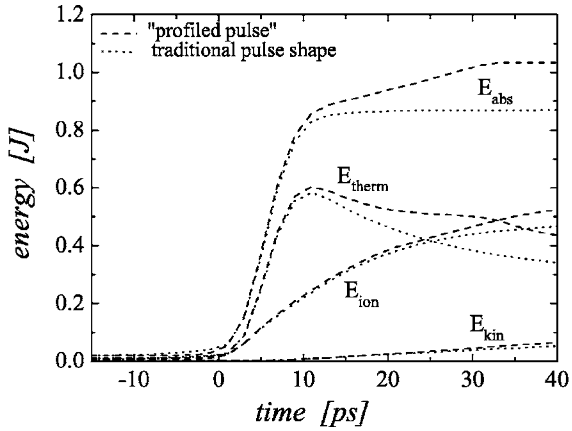

FIG. 3. The history of the energy partition (absorbed energy E_{abs}, thermal energy E_{therm}, ionization energy E_{ion}, and kinetic energy E_{kin}) in a plasma heated by pulses with two profiles: with steep edges (without pedestal sketched with the dotted lines) and including a trapezoidal pedestal with a very low background (dashed lines). The radiative energy has been neglected due to low level. Here "0" on the time axis corresponds to the peak of the heating pulse.

character, and the length of the output pulse indicating rather long-lived gain typical for the quasi-steady-state (QSS) systems.

An original locally-developed OPA third-order correlator with the dynamics about 10^5–10^6 works on the basis of difference frequency mixing. This correlator was applied to contrast measurements on the output pulse of a glass laser system. The first results of the measurements on the pulse contrast of our laser system were presented in Ref. [9]. It became clear from these measurements that the real amplified pulse cannot be correctly described by a simple two-step structure. The pulse correlation trace presented in Fig. 1 shows a typical nanosecond background at the intensity level of $(2-3)\times 10^{-3}I_{\max}$ and an additional pedestal with $I\sim 6\times 10^{-2}I_{\max}$. This pedestal with a width of $\sim$30 ps increases the pulse energy, if compared to the "clean" double pulse structure, by about 200 mJ and is especially well pronounced on the falling edge of the heating laser pulse. Such a pump pulse shape can be approximated by the profile drawn with the solid line in Fig. 2. The kinetics of the active medium created by pump pulses of different shapes was simulated using the hydrodynamics/atomic physics code EHYBRID used also in the simulations described in Ref. [4]. We have focused our interest on the temporal history of gain and partition of the energy deposited in the plasma. In modeling, a total energy of 1.6 J included in the laser pulse was focused into a line with a length of 6 mm and a width of 80 μm. The laser pulses were modelled by a combinantion of three components extracted in the real pulse shape shown in Fig. 1. A long Gaussian pulse with a rise time of the leading edge of 2 ns and a width of 2 ns (FWHM) was overlapped by a Gaussian pedestal with a width of 30 ps and finally by a heating Gaussian pulse with a width of 6 ps (FWHM) and a rise time of the leading edge of 6 ps (to the top). Relations between the peak intensities of those components were normalized to the peak intensity of the heating pulse and reflected the real

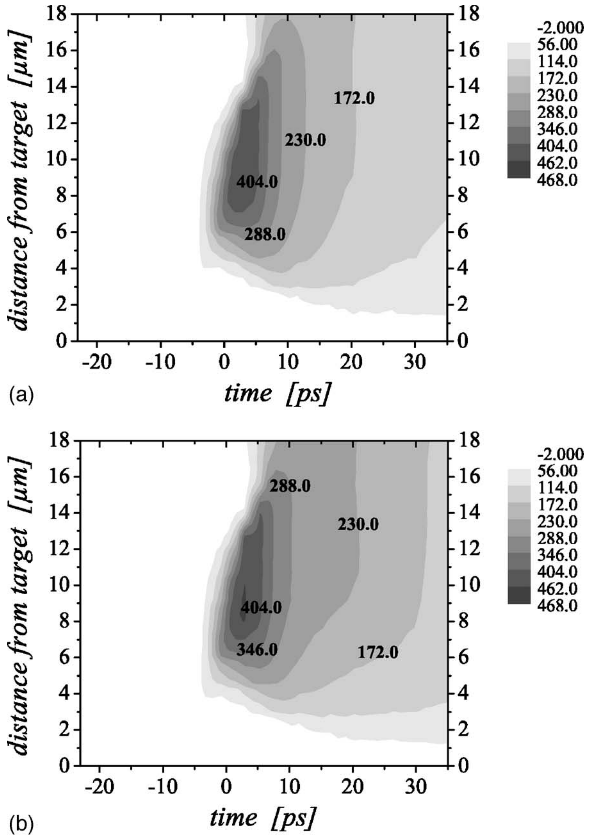

FIG. 4. The modeled spatiotemporal evolution of the electron temperature in an Ag plasma containing abundance of Ni-like ions and created by pulses with two profiles: (a) with steep edges and (b) including a trapezoidal pedestal. Here "0" on the time axis corresponds to the peak of the heating pulse and the temperature values are given in electronvolts.

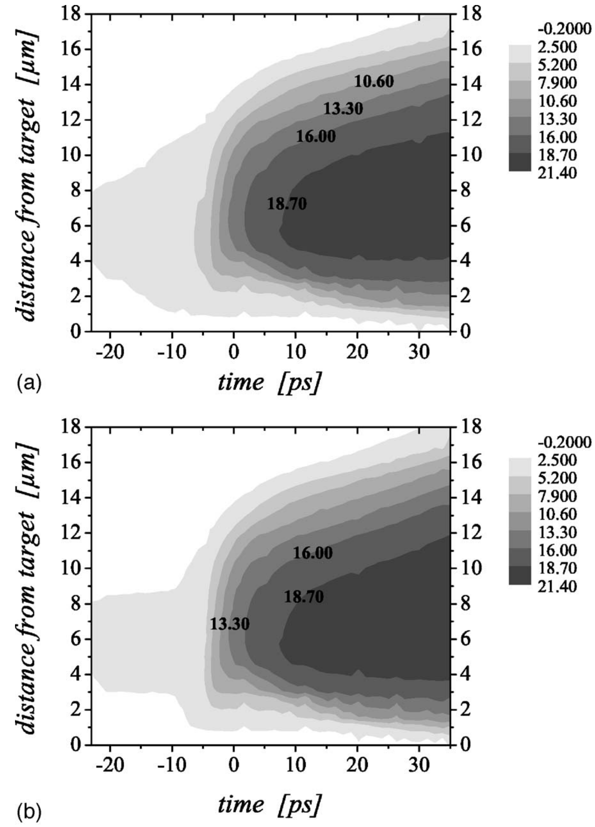

FIG. 5. The modeled spatiotemporal evolution of the average ionization stage in an Ag plasma containing abundance of Ni-like ions and created by pulses with two profiles: (a) with steep edges and (b) including a trapezoidal pedestal. Here "0" on the time axis corresponds to the peak of the heating pulse and the ionization stage is given in arbitrary units.

values presented in Fig. 1. The pump pulse profiles shown in Fig. 2 have been sketched to distinguish and pronounce some features present in the shape of the real pump pulse at low signal level, and to show their influence on the active medium kinetics. Significant differences between the pulse shapes were seen at an intensity level well below $0.1I_{\max}$. Figure 2(b) shows the zoomed low-level structure of the pumping laser pulses shown in Fig. 2(a). The shape drawn with the solid line corresponds well to the original measured pulse profile. The dotted line sketches a pulse representing parameters typical for the traditional double-pulse technique; i.e., low-energy background and a heating pulse that is very steep at both edges. Two other profiles [dashed and dash-dotted lines in Fig. 2(b)] had, for the sake of simplicity, trapezoidal pedestals on the trailing edge with different peak intensities and different background levels. Different line styles refer to different pulse structures and this relation is kept over all figures. The absorbed part of the energy incident on the target is distributed among different energy components that behave differently in time. From the kinetics point of view, the thermal energy (energy of translational movement of free particles, here mainly electrons) responsible for the excitation process is of crucial importance. Figure 3 shows the calculated temporal changes in the energy partiton for two distinctly different pulse shapes among those presented in Fig. 2 (dashed and dotted lines). The dotted lines in Fig. 3 reflect changes of energy components for the two-step pulse with a very limited energy contained out of the main heating pulse (corresponds to the traditional double-pulse scheme). The dashed lines correspond to one of the shapes modeled with a trapezoidal pedestal on the trailing edge of the pump laser pulse and the lower background. It is seen that the low-level background combined with the steep edges of the short pulse (dotted line) very quickly stabilizes the absorbed energy, and the thermal energy decays monotonically after its maximum as a consequence of the cooling process. A small amount of the preplasma was created in this case and the plasma temperature resulted from the competition between collisional absorption and cooling. In contrast, the pulse with the pedestal works in a similar way only up to the point corresponding closely to the pump pulse peak. After that the absorbed energy still increases and stabilizes its value at the end of the pedestal. The amount of energy absorbed changes notably even if a very limited energy is delivered in the pedestal of the incident laser pulse. The presented results suggest that up to 80% of the energy included in the pedestal can be absorbed. At the same time the thermal energy (temperature) of the created small plasma plume initially decreases due to efficient cooling. However,

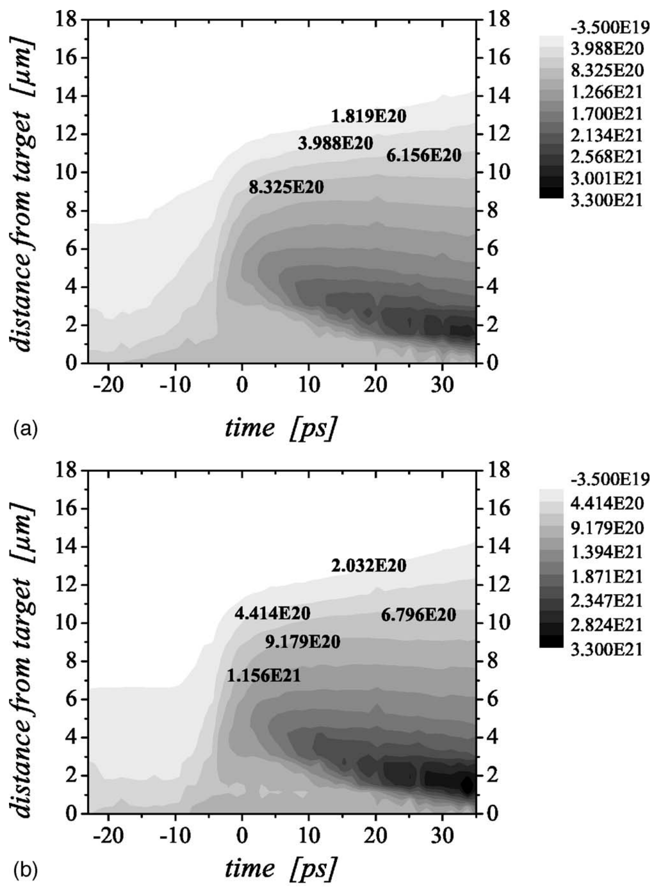

FIG. 6. The modeled spatiotemporal evolution of the electron density in an Ag plasma containing abundance of Ni-like ions and created by pulses with two profiles: (a) with steep edges and (b) including a trapezoidal pedestal. Here "0" on the time axis corresponds to the peak of the heating pulse and the density unit is $[\mathrm{cm}^{-3}]$.

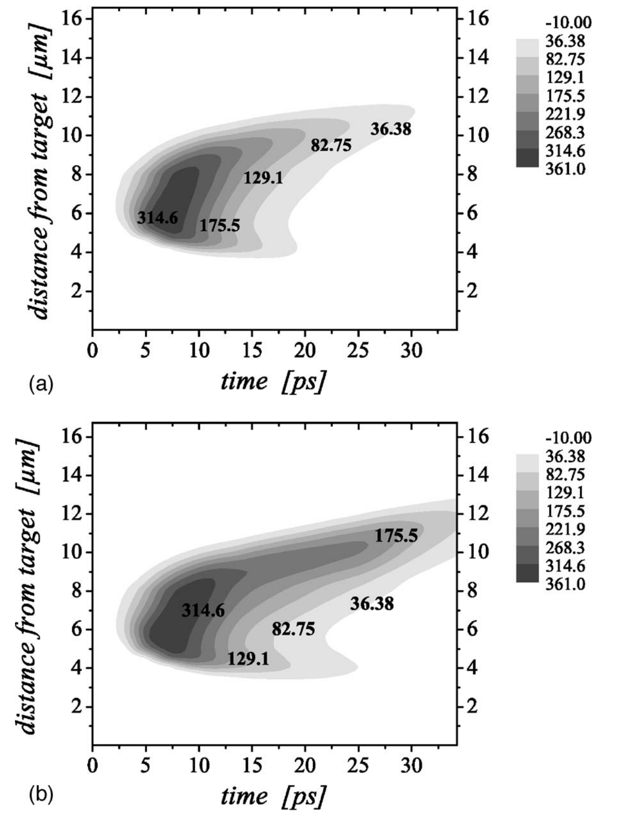

FIG. 7. The modeled spatiotemporal evolution of the local gain coefficient at 13.9 nm in a plasma with an abundance of Ni-like Ag ions produced by pulses with two profiles: (a) with steep edges and (b) including a trapezoidal pedestal. Here "0" on the time axis corresponds to the peak of the heating pulse. The gain coefficient is given in $[\mathrm{cm}^{-1}]$.

when a sufficient amount of the thermal energy from the pedestal is accumulated, cooling will be inhibited and the decay of the thermal energy in Fig. 3 converts into the plateau. Further decay of the thermal energy begins directly after the stabilization of the absorbed energy; i.e., when no more energy is delivered to the plasma. The surprisingly small amount of pump energy delivered in the pedestal of the pump pulse is already decisive for the excitation process as the described feature influences noticeably the energy partition in the medium. The thermal energy of the medium increases on a short time scale, inhibiting for some time cooling of the medium. Additionally, the ionization energy increases slightly at the end of the ramp of the absorbed energy when the pedestal is present. This implies a limited increase in the average ionization stage due to the reheating process. (Compare E_{therm} and E_{ion} traced with different line styles in Fig. 3.) Relying on this analysis, we assume that may be because the gain is formed slightly further out in the corona as the plasma ionizes up to the nickel-like stage, with the extra energy from the pedestal deposited in this region the gain would be allowed to develop preferably there. To validate this scenario we have traced contour plots showing spatio-temporal evolution of the most important plasma parameters such as plasma temperature T_e (Fig. 4), average ionization stage Z^* (Fig. 5), and plasma density n_e (Fig. 6) for both pump pulse shapes, i.e., with and without the pedestal. The results definitely confirm our assumption and proposed scenario of the gain development. It is seen that due to deposition of the additional energy in the area positioned further from the target the region with an increased electron temperature has been significantly extended [compare Figs. 4(a) and 4(b)]. As the average ionization stage has also slightly increased in the same area (Fig. 5), the region with the conditions favorable for the gain buildup is noticeably extended. The changes in the plasma density distribution are negligibly small. The evolution of the plasma parameters is very smooth and the differences are clearly seen only by quantitative comparisons. The final effect of the observed changes can easily be observed in Fig. 7, where spatiotemporal evolution of the local gain coefficient has been plotted. While there is no noticeable spatial shift of the high gain area, the gain duration becomes significantly longer in the outer region of the medium. This is exactly the expected effect of the additional heating by the pedestal energy. As a consequence of reheating, the cold absorption domain, usually spreading outward in the plasma plume in the scheme with a "clean" (without pedestal) single heating pulse, disappears here. The longer the pedestal on the trailing edge, the

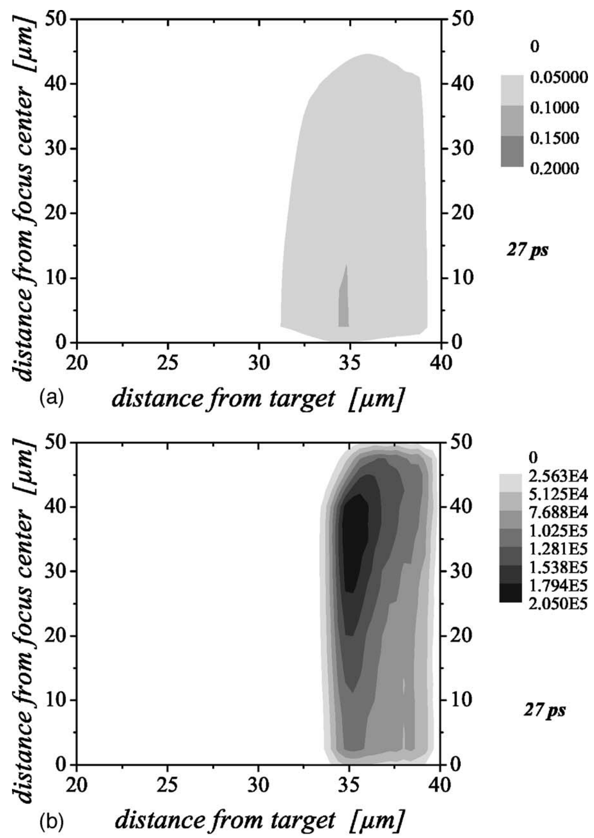

FIG. 8. Modeled near-field spot of the x-ray beam at 13.9 nm obtained by pumping: (a) with steep edges and (b) including a trapezoidal pedestal. Please note that the maximum intensity in (a) is still six orders of magnitude lower than that in plot (b). The snapshots correspond to the situation 20 ps behind the gain peak (27 ps behind the peak of the heating pulse).

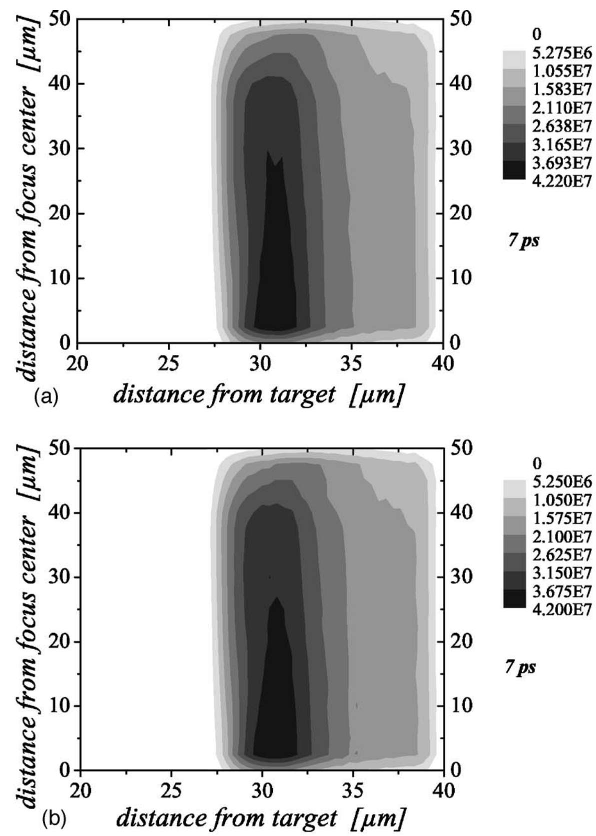

FIG. 9. Modeled near-field spot of the x-ray beam at 13.9 nm obtained by pumping: (a) with steep edges and (b) including a trapezoidal pedestal. Similarity of the spot shapes is evident. The snapshots correspond to the situation 7 ps behind the peak of the heating pulse, i.e., at the moment of the gain peak.

longer is the deposition of the additional energy. The most evident proof of the processes described are changes in the near-field profiles of the radiation emitted in both cases. The area with a long-lived gain promotes stronger other group of rays in the amplification process. This change is dramatic and is seen in Fig. 8, where the near-field spots are traced for the moment delayed by 27 ps relative to the peak of the heating laser pulse or 20 ps behind the gain maximum. Both spots are drawn at a different intensity level for the sake of comparison but the difference is evident. The output of the medium pumped with the pulse with the pedestal is by 6 orders of magnitude stronger than that without the pedestal. The plots in Fig. 8 give a sort of output snapshot for the plasma conditions existing at this moment. Figure 8(b) also shows a strong influence of refraction in the plane parallel to the target surface at the late phase of the gain development. For the sake of comparison, Fig. 9 shows the near-field spot at the moment of the gain maximum (delayed 7 ps relative to the peak of the heating laser pulse). The spot shapes and the intensity levels are very similar. The consequences of the kinetic processes and the influence of the profiled pump pulse on the history of the buildup of the population inversion in the medium are clearly seen in Fig. 10. The history of the maximum local gain factor is drawn there for the different pulse shapes shown earlier in Fig. 2. It has to be stressed, that all these lines are not related to a fixed position relative to the target but the spatial shift of the maximum gain is minimal, as discussed earlier. The pulse with no pedestal, resembling the double-pulse pump configuration (dotted line) does not bring significant changes to the temporal shape of the gain in comparison to that reported in Ref. [4]. The FWHM of the gain curve is between 10 and 15 ps and changes very weakly with the length of the pump pulse. This resistant behavior of the gain lifetime against the pump pulse length was also observed in the double-pulse experiments [8]. This variant of the pump process gives a high but short-lived gain. Such a behavior is understandable as a small amount of the plasma created by a background radiation at the beginning phase of the heating pulse (background level) is efficiently heated by a low-energy main picosecond pump pulse. However, the small plasma plume created in this way is easily cooled by thermal conduction to the massive bulk material of the target. Increase in the prepulse energy results in the increase of the amount of the ablated material, and hence also in reduction in the plasma temperature and finally in lower gain. This increase of the prepulse energy could be caused by the increase in the background level or appearing of an additional pedestal in front of the heating pulse. This can be easily deduced if dotted and dashed lines in Fig. 10

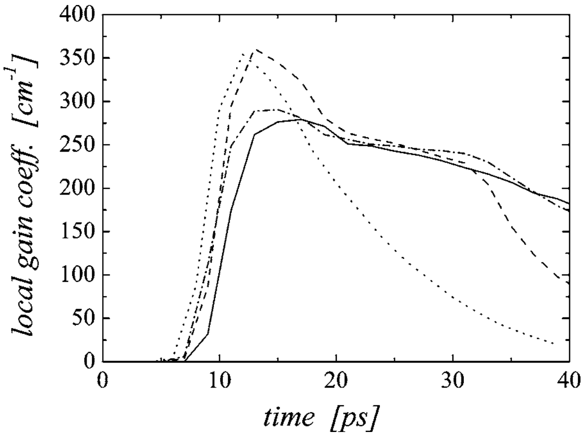

FIG. 10. The gain history of the maximum local gain for different pump pulse structures. Here "0" on the time axis corresponds to the peak of the heating pulse. The line styles used corresopond to the pulse shapes sketched in Fig. 2. Solid: the real measured pulse shape, dot: without any pedestal (corresponding to the traditional shape in double-pulse scheme), dashed: trapezoidal pedestal and very low background lasting 4 ns, dash-dotted: trapezoidal pedestal and stronger background lasting 4 ns.

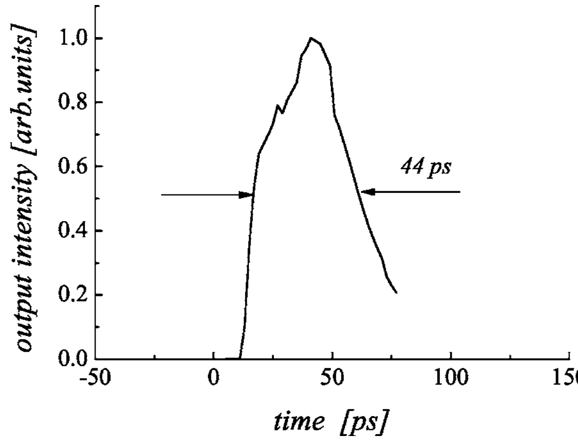

FIG. 11. Temporal shape of the output XRL pulse in far-field modeled with EHYBRID. Here "0" on the time axis corresponds to the peak of the heating pulse.

(higher gain) are compared with the pulse shapes plotted in Fig. 2(b) with the same lines. Higher gain coefficient corresponds to significantly lower background, i.e., smaller plasma plume. On the other hand, if some pronounced pedestal or hump has appeared on the trailing edge of the pump pulse the peak gain factor is only slightly (by ~20%) reduced but the gain lifetime is extended dramatically (Fig. 10). An energy as low as 200 mJ delivered within 20 ps after the main heating laser pulse, increases lifetime (FWHM) of the gain to about 50–60 ps, and cancels the exponential character of its decay. Interestingly, reduced steepeness of the pedestal falling edge increases the gain lifetime as well (see solid line in Fig. 10). The scale of the effect is even more evident in Fig. 11. This figure shows a temporal shape of the output pulse in far-field modeled in the unidirectional approximation with the RAYTRACE code developed at York [11]. An estimated FWHM value of 44 ps corresponds very well with the values observed in the experiments. These values were scattered between 27 and 46 ps and were strongly dependent on the pump conditions. The quoted earlier experimental value of 32±3 ps was derived from few shots under identical pump conditions. A value of 36±10 ps would probably be more reasonable. Taking into account some idealized conditions and assumptions in modelling we found the agreement fairly satisfactory. In this way a sort of reconciliation between two different regimes (transient and QSS) became a fact. The Ni-like silver XRL pumped by a single profiled laser pulse showed gain lower than that available in the traditional double-pulse irradiation but still very high and long lived. The latter is on a scale characteristic rather for the QSS working regime. With the gain lifetimes observed in the simulations, the output pulse length of about 30 ps recorded in the experiment becomes understandable, and the limited increase in the gain factor under pumping with the traveling-wave arrangement is also consistent with this result.

In summary, on the basis of plasma kinetics we have explained the apparent contradiction between the high gain and its long-lived character observed in the experiments on Ni-like soft x-ray lasers pumped by a single picosecond profiled pulse. Pulse profiles recorded in the experiments differed significantly from a simple picture of the traditional arrangement [1,4,10]. It was found that the shape of both edges determines conditions of plasma heating and hence also the history and the level of the gain. The leading edge of the pulse and especially its low-level background decide about the peak gain value. On the other hand, the trailing edge of the heating pulse determines the cooling conditions (distribution of the deposited energy) and also constitutes a decisive factor in the gain lifetime. These fundamentals can be the starting point in further optimisation of the pumping process by controlled active shaping of the pump pulse.

We are very grateful to Geoff Pert of the University of York for encouragement and valuable discussions in connection with the work presented here as well as to Howard Reiss, a Guest Professor at MBI, for his contribution to improvement of the manuscript quality.

[1] J. Dunn, A. L. Osterheld, R. Shepherd, W. E. White,V. N. Shlyaptsev, and R. E. Stewart, Phys. Rev. Lett. **80**, 2825 (1998).

[2] J. Dunn, Y. Li, A. L. Osterheld, J. Nilsen, J. R. Hunter, and V. N. Shlyaptsev, Phys. Rev. Lett. **84**, 4834 (2000).

[3] K. A. Janulewicz, A. Lucianetti, G. Priebe, W. Sandner, and P. V. Nickles, Phys. Rev. A **68**, 051802(R) (2003).

[4] K. A. Janulewicz, P. V. Nickles, R. E. King, and G. J. Pert,

Phys. Rev. A **70**, 013804 (2004).
[5] J. Dunn *et al.*, in *Proceedings of the 7th IXRLC in St. Malo "X-Ray Lasers 2000*," France, 2000, edited by G. Jamelot, C. Mller, and A. Klisnick (EDP Sciences, Les Ulis, 2000); J. Phys. IV France **11**, Pr2-19 (2000).
[6] K. A. Janulewicz *et al.*, in Proc. SPIE **5197**, 90 (2003).
[7] K. A. Janulewicz *et al.*, in *Proceedings of 8th International Conference on X-Ray Lasers*, Aspen, 2002, edited by J. J. Rocca, J. Dunn, and S. Suckewer, AIP Conf. Proc. No. 641, AIP, Melville (2002), p. 26.
[8] J. Dunn *et al.*, Proc. SPIE **5197**, 51 (2003).
[9] K. A. Janulewicz, J. Tümmler, G. Priebe, and P. V. Nickles, IEEE J. Sel. Top. Quantum Electron. **10**, 1368 (2004).
[10] S. Maxon *et al.*, Phys. Rev. Lett. **70**, 2285 (1993).
[11] J. A. Plowes, G. J. Pert, S. B. Healy, and D. T. Toft, Opt. Quantum Electron. **28**, 219 (1996).